Why Cyanide Pretends To Be A Weak-Field Ligand In $[Cr(CN)_5]^{3-}$

Richard Lord

Advisor: Prof. Mu-Hyun Baik

C500 Final Report

April 21, 2006

I. Introduction and Research Goals

Transition metal complexes that exhibit spin-crossover behavior are of great interest due to their key role in biological processes[1] and their potential applications in materials chemistry as electronic and magnetic molecular devices.[2] One of the most extensively studied examples of spin-crossover occurs in cytochrome P450 enzymes.[3] Upon binding a substrate, the metal center of the heme unit is oxidized from Fe(II) to Fe(III) and the metal adopts a high-spin d^5 configuration. Throughout the remaining mechanistic steps, the electronic configurations are toggled to optimize the redox properties which control reaction rates and product distributions. Many fundamental issues remain to be resolved because to date there is no systematic understanding of the electronic features governing spin-state equilibria.

Before tackling such a complex system, we wanted to explore the intrinsic properties of transition metal complexes that influence the electronic configuration. The homoleptic complex anion $Cr^{II}(CN)_5^{3-}$ was recently shown to exhibit magnetic properties that are only consistent with a high-spin Cr(II) d^4 center, where all four metal-based electrons are unpaired.[4] This observation is quite striking because cyanide ligands are widely accepted as strong-field ligands, which predicts a low-spin configuration for Cr(II) with a maximum of two unpaired electrons at the metal center. Interestingly, presence of K^+ ions instead of the non-coordinating counter ion NEt_4^+ affords the complex anion $Cr^{II}(CN)_6^{4-}$.[5] A low-spin configuration is displayed for this complex ion-pair, in much better agreement with intuitive expectations. This problem provides an ideal entry into a number of fundamental issues in spin-crossover systems containing transition metals:

(i) Why is $Cr^{II}(CN)_6^{4-}$ unstable in the presence of NEt_4^+? Is Cr(II) simply incapable of supporting six anionic ligands with relatively localized charge, or is there a more complicated explanation?

(ii) What is the relationship between the molecular structure and relative spin-state energies? M–L bond distances, as well as coordination geometry, must significantly influence the electronic configuration; can we quantify these effects?

(iii) What role does the counter ion play on spin-state equilibria? Also, how does the system respond to the perturbation of counter ion addition? Does this lead to a simple electrostatic interaction, or are the electronics significantly influenced?

(iv) Is DFT an appropriate choice of model chemistry to describe spin-state equilibrium in transition metal complexes?

Our choice of DFT over multi-determinant methods was primarily due to the efficiency of DFT allowing it to handle the larger ligands present in many transition metal systems exhibiting spin-crossover, which we plan to study in the future. This small system provided a perfect platform to assess whether or not DFT could *qualitatively* reproduce the physical picture. B3LYP, one of many available DFT functionals, has performed reasonably well for transition metal containing systems to date.[6] Unfortunately, systematic benchmarks of DFT methods for realistically complex spin-crossover systems are not available. A major portion of my ongoing research includes extensive testing of model

chemistries to determine which (if any) are suitable for *quantitatively* describing spin-crossover.

II. Methods

All calculations were carried out using DFT as implemented in the Jaguar 6.0 suite of *ab initio* quantum chemistry programs.[7] Geometry optimizations were performed at the B3LYP/6-31G** level of theory,[8-11] with transition metals represented using the Los Alamos LACVP basis that includes relativistic effective core potentials, unless otherwise noted.[12-14] Herein this level of theory will be denoted B3LYP/LACVP**. Following the computational protocol previously established by our group,[15] energies of optimized structures are recomputed by additional single-point calculations using Dunning's correlation-consistent triple-ζ basis set cc-pVTZ(-f).[16] For all transition metals, we use a modified version of LACVP, designated as LACV3P, where the exponents were decontracted to match the effective core potential with a triple-ζ quality basis. Solvation energies for molecules were computed using a continuum solvation model, with dielectric constants of 78.4 and 37.5 for water and acetonitrile, respectively. Solvation energies and vibrational calculations were computed at the B3LYP/LACVP** level of theory. All stationary points were confirmed to be minima by checking the harmonic frequencies. Thermodynamic properties and redox potentials were calculated as calibrated by Baik and Friesner, summarized below:[15]

$$\Delta H^{EA}(\text{gas}) = \Delta H^{EA}(\text{SCF}) + \Delta ZPE + \Delta H^{T} \quad (1)$$

$$\Delta G^{EA}(\text{gas}) = \Delta H^{EA}(\text{gas}) - T\Delta S(\text{gas}) \quad (2)$$

$$\Delta G^{EA}(\text{sol}) = \Delta G^{EA}(\text{gas}) + \Delta G^{solv} \quad (3)$$

$$\Delta G^{EA}(\text{sol}) = -nFE^{0} \quad (4)$$

III. Results and Discussion

For all discussions about Cr(II) herein, high-spin will refer to the S=2 configuration with four unpaired electrons and low-spin will refer to the S=1 configuration with two unpaired electrons. A first approximation to the electronic structure for each of the geometries (octahedral, square planar, and trigonal bipyramidal) are displayed in Figure 1.

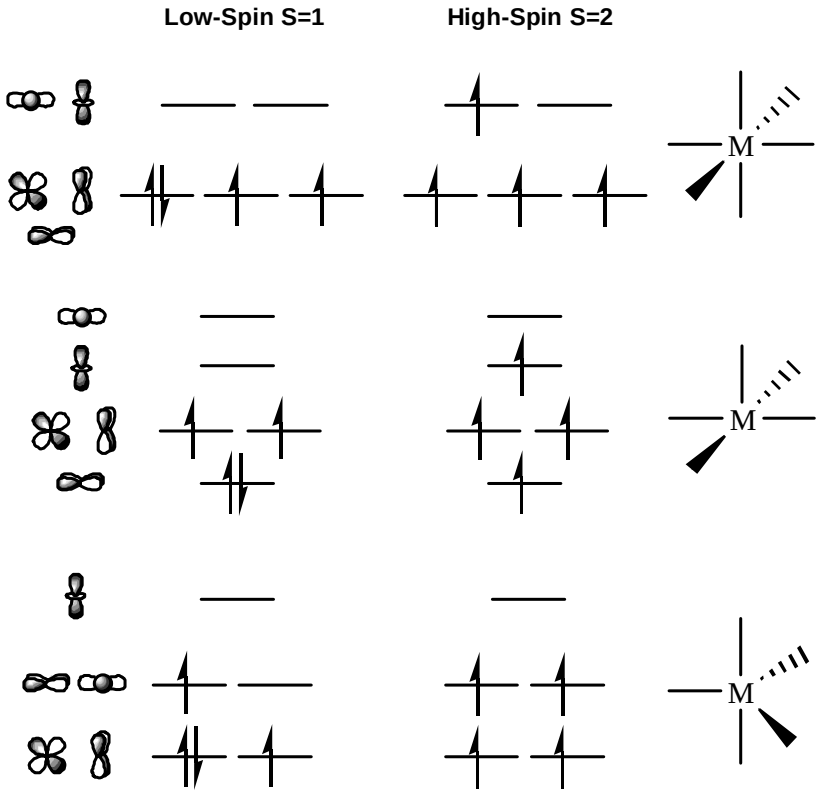

Figure 1. Ideal σ-ligand only orbital splitting diagrams for an octahedral, square planar, and trigonal bipyramidal coordination geometry, respectively.

Compound	ΔG(gas phase) / kcal/mol	ΔG(solv) / kcal/mol
Low-Spin Octahedral $Cr(CN)_6^{4-}$	0.00	0.00
Low-Spin Trigonal Bipyramidal $Cr(CN)_5^{3-}$	-196.69	-4.91
High-Spin Trigonal Bipyramidal $Cr(CN)_5^{3-}$	-220.21	-26.96
Low-Spin Square Pyramidal $Cr(CN)_5^{3-}$	-190.16	-7.69
High-Spin Square Pyramidal $Cr(CN)_5^{3-}$	-218.92	-25.46

Table 1. Thermodynamics of cyanide ligand dissociation.

Formation of the hexacyano complex was found to be thermodynamically unfavorable, both in the gas phase and with implicit solvent, as shown in Table 1. These calculations also suggest that a high-spin structure with six bound cyanide ligands is not feasible. This observation can be rationalized by recognizing that the d_{z^2} antibonding orbital is being populated in the high-spin configuration. All calculations using different initial geometries quickly displayed ligand dissociation to give the square pyramidal structure.

Because these complexes are highly anionic in nature, the potential energy surfaces were also explored after augmenting the triple-ζ basis set with two sets of diffuse functions. Results for most of the species were questionable, likely due to the lack of a properly calibrated numerical grid in the Jaguar 6.0 suite, and therefore the results at the

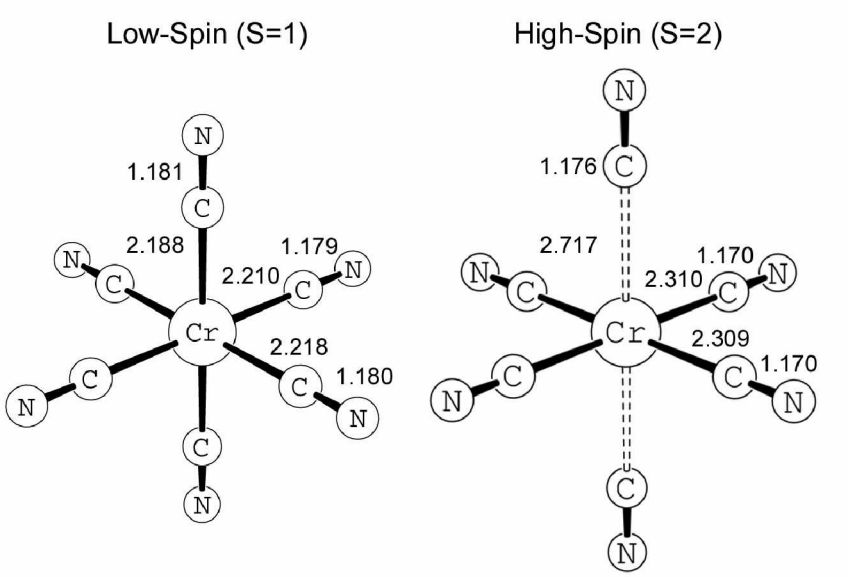

Figure 2. Structures for the low-spin complex and high-spin hexacyanochromate(II) transition state. Bond lengths are in Å.

LACVP** basis were assumed to be more reliable. Importantly, no additional minimum with six bound cyanide ligands was located on the high-spin potential energy surface. The symmetric cyanide dissociation transition state to produce a square planar high-spin tetracyanochromate(II) species,

however, was located and is shown above in Figure 2, along with the minimum for the low-spin structure at the B3LYP/LACVP** level of theory.

In Figure 2 we see that low-spin $Cr(CN)_6^{4-}$ experiences Jahn-Teller distortion to give a D_{2h} structure, due to asymmetric occupation of four electrons in the t_{2g} orbitals. The Cr–CN distances are 2.188, 2.210, and 2.218 Å. From the high-spin $Cr(CN)_6^{4-}$ dissociation transition state in Figure 2, we see elongated Cr–CN bond lengths of 2.309 and 2.310 Å for the bound cyanides, which can be attributed to fewer electrons in the t_{2g} space orbitals to π-backbond to the cyanide. This is further supported by comparing the cyanide C–N bond distances with those of dissociating cyanide, or free cyanide, which

were calculated to have bond lengths of 1.176 and 1.184 Å, respectively. Metal–cyanide bond distances of this magnitude are unusual given the overwhelming evidence for significantly shorter bond lengths (1.89-2.08 Å) in typical homoleptic cyano complexes involving a divalent metal.[17] Interestingly, Nelson *et al*. observe similarly elongated Cr–CN bond lengths in the $(NEt_4)_3[Cr(CN)_5]$ crystal structure, ranging from 2.11-2.23 Å.[4]

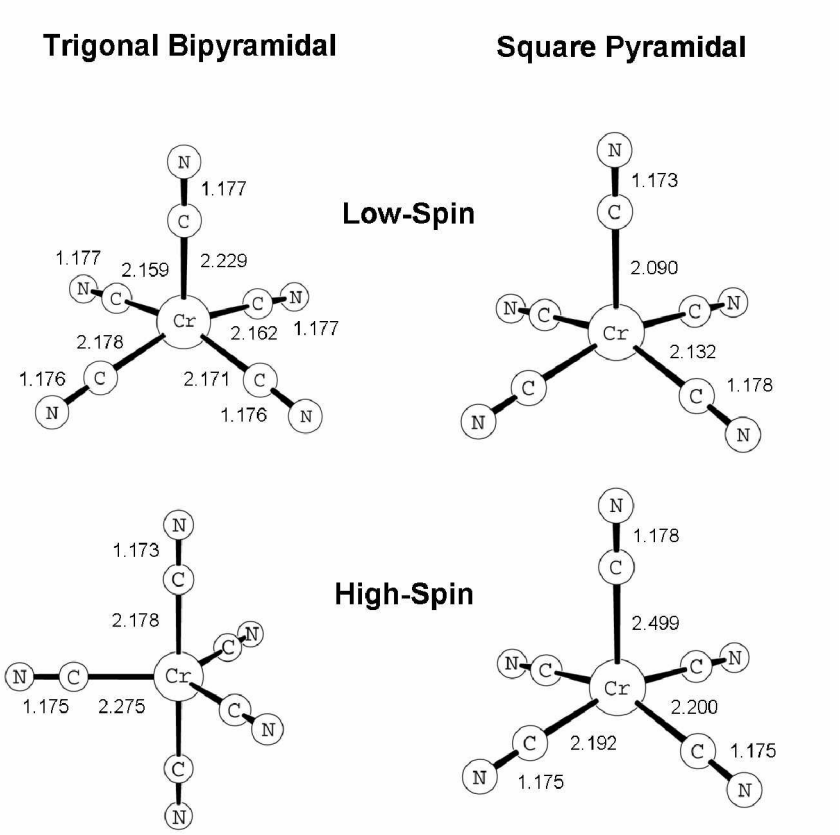

Figure3. Structures for the low-spin and high-spin pentacyanochromate(II) complexes. Bond lengths are in Å.

Structures for the pentacyano complexes are summarized in Figure 3. The low-spin minimum structure for the trigonal bipyramidal structure was found to undergo a large distortion due to the simultaneous asymmetric occupation of the degenerate d_{xz} / d_{yz} orbitals, and the degenerate $d_{x^2-y^2}$ / d_{xy} orbitals, as seen in the first-order approximation of

Figure 1. Therefore, both of the low-spin structures are pseudo square planar while a distinct trigonal bipyramidal and square planar structure were located on the high-spin potential energy surface. Bond lengths agree reasonably well with those reported by Nelson and co-workers,[4] as these calculations do not capture distortions due to packing in the crystal structure. Analogous to the hexacyano complexes, Cr–CN bond distances are much longer than one would predict.

It is clear that the Cr–CN bond distances provide important clues about the electronic nature of these systems. We hypothesized a "charge-overload" effect may be operative, whereby chromium is unable to support six highly anionic ligands in its divalent state, mainly due to Coulombic repulsion. As a gedanken experiment, a model was developed to quantify the effect of Cr–CN ligand distance on the spin-equilibrium. Single point calculations at the B3LYP/cc-pVTZ(-f) level of theory mapped the potential-energy surface as a function of this Cr–CN distance for both the low- and high-spin complexes in

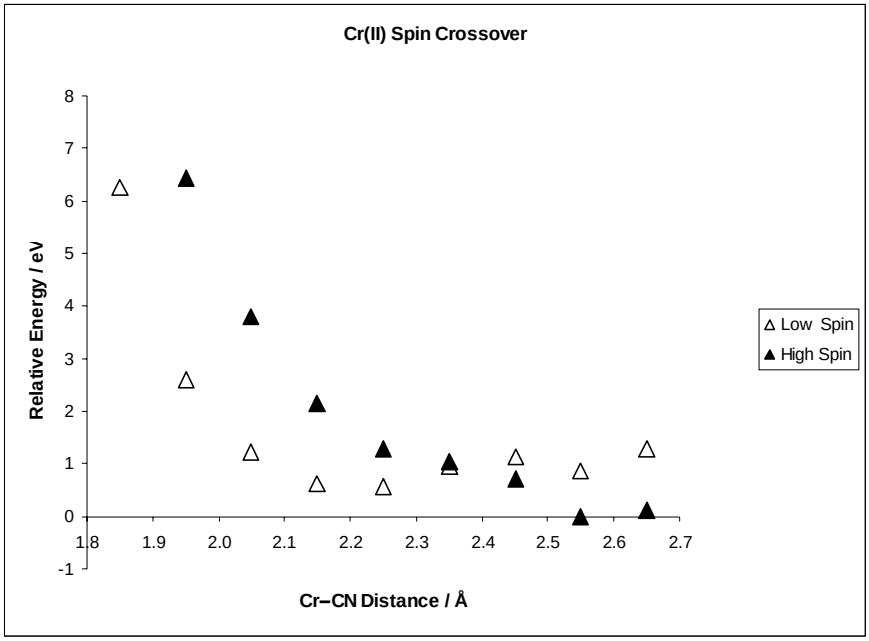

Figure 4. Electronic energy as a function of the Cr–CN distance for both the low- and high-spin configurations.

a perfect octahedral environment. Cyanide bond lengths were taken from the minima and frozen at values of 1.180 and 1.170 Å for the low- and high-spin complexes, respectively. Results of this study are summarized in Figure 4.

At short bond distances, the low-spin configuration is favored due to a parametric dependence of d orbital splitting on the metal-ligand orbital overlap. Near 2.35 Å, the two surfaces are predicted to cross. While this value for a spin-crossover event is not exact, it does give us an excellent first-order approximation to where such an event might be feasible, and coincides well with Nelson and co-workers' experimentally observed, and our predicted, bond lengths.[4] In the absence of an octahedral ligand environment, the spin-crossover event would occur at a shorter Cr–CN bond distance due to fewer σ-donor ligands interacting with the metal based d orbitals. This explanation matches quite well with our hypothesis of "charge-overload". Based purely on electrostatics, the six highly anionic ligands overwhelm the positive, divalent chromium leading to much longer than expected bond lengths.

If "charge-overload" is the controlling factor, it is reasonable that Fe(II), another well known low-spin complex as an alkali salt,[17] should also experience a similar force and adopt an unexpected high-spin configuration in the presence of non-coordinating counter ions. A quick search of the crystal structure database[18,19] revealed many known Fe(II) complexes in the presence of non-coordinating anions. Representative complexes have classical homoleptic cyano bond lengths close to 1.92 Å.[20-28] While no study confirmed the spin-state, these bond lengths are only sensible for the low-spin electronic configuration, as indicated in the calculations discussed below. Figure 5 shows the energies of the HS and LS complexes as a function of Fe–CN distances.

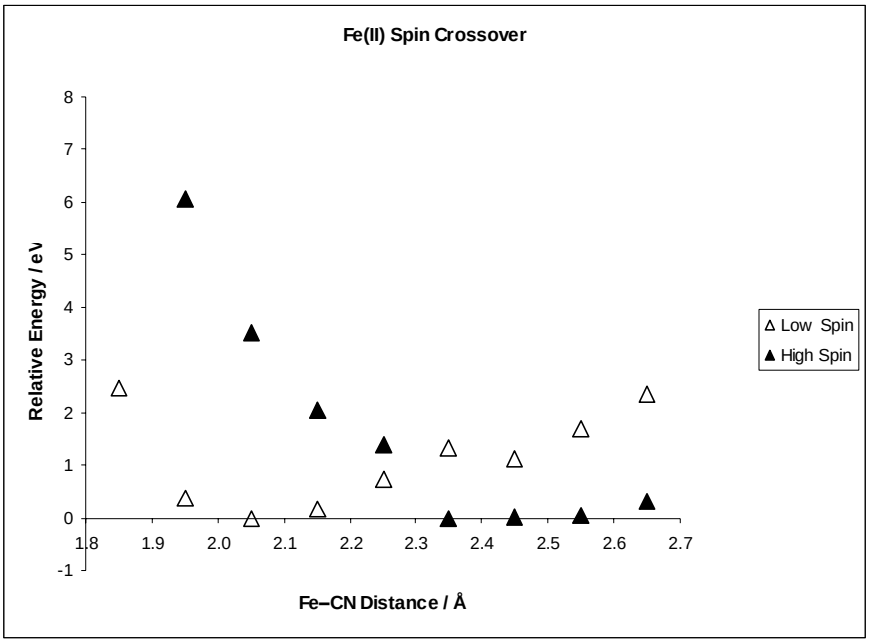

Figure 5. Electronic energy as a function of the Fe–CN distance for both the low- and high-spin configurations.

Again we predict spin crossover to occur in the region where the M–CN distance approaches 2.30 Å, however, the picture painted in this case is dramatically different. For Fe(II), the minima for the two spin state surfaces are now much deeper, the energies of the minima are nearly isoenergetic on the electronic energy surface, and the minimum-minimum separation has increased by nearly 0.1 Å when compared to the results for Cr(II). It is worth noting that the Fe–CN bond lengths are longer than those experimentally observed by about 0.1 Å.

Confronted with this result which seems to contradict our hypothesis that "charge-overload" is the dominant factor for the observation of high-spin Cr(II), we decided to look at the sizes of the metals as the electronic structure changes. Metal size will be important in determining how well it can support anionic ligands in a simple electrostatics model. For low-spin atomic configurations, one expects Fe(II) to be smaller than Cr(II)

due to additional electrons in the t_{2g} space capable of backbonding. This reduced size leads to more localized cationic charge on the metal center, which is better suited to support the electrostatic demand of the anionic ligands. High-spin Fe(II) on the other hand has two unpaired electrons in the e_g space, compared to the one unpaired electron of Cr(II), which through antibonding interactions leads to a larger metal center less capable of handling the excess charge of the six cyanides. From this emerges a complicated picture where both the electronics and charge are in a careful balance, and both effects are not entirely separable.

Because the alkali salts of $Cr(CN)_6^{4-}$ are well known, we decided to explore the

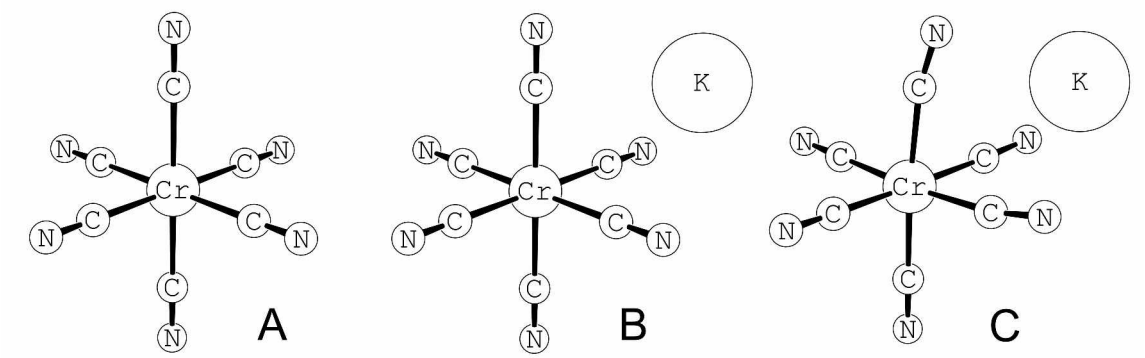

Figure 6. Structural change upon introduction of a potassium ion into the coordination sphere of $Cr(CN)_6^{4-}$.

	LS / kcal/mol	**HS / kcal/mol**
Electrostatics (B-A)	-310.88	-276.91
Relaxation (C-B)	-66.55	-66.02
Overall (C-A)	-377.43	-342.93

Table 2. Electronic energy differences in the energy decomposition between electrostatics and structural relaxation upon introduction of K^+.

effect of introducing coordinating K^+ ions to further probe the connection between the "charge-overload" on the metal center and spin-state equilibrium. Not surprisingly, addition of K^+ stabilized the more compact low-spin complex more than the high-spin complex. However, we wanted to quantify the nature of this stabilization and decided to partition the relaxation into its electrostatic and structural components. By artificially bringing the K^+ into its equilibrium position relative to the Cr(II) center, a single point calculation was evaluated to measure the magnitude of these effects on the electronic energy. These energies and structures can be found in Table 2 and Figure 6, respectively.

Electrostatic relaxation emerges as the dominant factor in stabilizing the low-spin state compared to the high-spin state. This serves to not only deepen the well which the low-spin state sits in, but also to thermodynamically increase the population of the low-spin state which can have six cyanides bound versus the high-spin state, in which one of the CN ligands dissociates. A shortening of the bond lengths is also observed, with Cr–CN bond distances of approximately 2.10 Å (Figure 6). Of course, a natural question arising from this analysis is: if ion-coordination is so vital to the stability of the low-spin state, would the solution structure include explicit ion-pairs? To help answer this last question, the redox potentials of many different species were calculated to see if the redox potential for $Cr(CN)_6^{4-}$ suggests the presence of these species.

Redox couples ($Cr(III) \rightarrow Cr(II) + e^-$) for all potassium salts up to the neutral species with four coordinated ions have been investigated. Experimentally, the reduction potential is observed to be between -1.383 and -1.521 V vs SCE.[29] Baik and Friesner described in a recent paper that redox potentials can be reliably predicted with our current

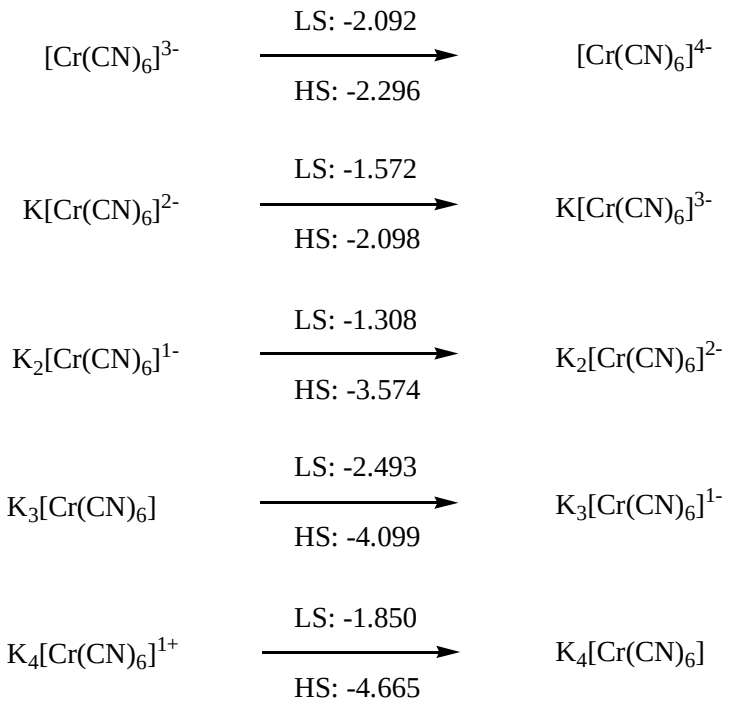

Figure 7. Redox potentials for the ion-pairs under aqueous conditions. Reported in V.

theoretical prescription giving accuracies (~150 mV) approaching those of experimental error.[15] Shown in Figure 7 are the predicted reduction potentials in water.

However, one can also imagine that more than a simple redox event is occurring on the timescale of the electrochemical measurements. The possibility of ion pairing to yield overall charge neutral electrochemical-chemical reactions was also probed, as shown in Figure 8.

From these data, the tandem electrochemical-chemical reactions do not appear to reproduce the experimental values within the expected error bars. In every case, the ion-

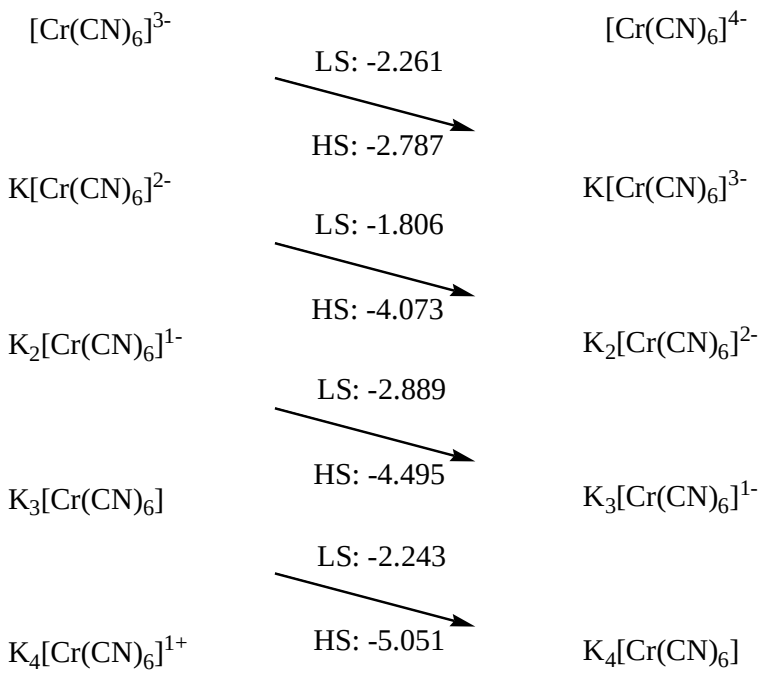

Figure 8. Redox potentials for the ion-pairs under aqueous conditions, probing for ion-pairing events on the same timescale. Reported in V.

pairing event decreases the spontaneity of the reaction. This observation is still being investigated. However, the mono- and dipotassium ion-pairs both exhibit electrochemical redox potentials in good agreement with the experimental redox potentials, seemingly confirming our hypothesis that ion-pairing must be critical to formation of the low-spin hexacyanochromate(II) complex in aqueous solution. It is still ambiguous as to which structure is actually competent in solution, or whether an equilibrium exists. Additional work to delineate this finding is in progress.

IV. Conclusion

Through this C500 project we have accomplished most of the goals we set out to explore including: (i) understanding the role of the counter ion in spin-state thermodynamics, (ii) quantifying the effect of M–L bond distance as well as coordination geometry on spin-state equilibria, (iii) harmonizing the observation of low-spin Cr(II) and high-spin Cr(II) when coordinating and non-coordinating counter ions are utilized, and finally (iv) the observation that B3LYP/cc-pVTZ(-f)//B3LYP/LACVP** seems to qualitatively reproduce the experimentally observed properties of this system quite well. We have also opened "Pandora's Box" when it comes to truly understanding how the different factors affecting spin-state equilibrium come together, as exemplified in the Cr(II)/Fe(II) discussion above. Additionally, more work on the electrochemistry may be warranted given the peculiar behavior of the electrochemical-chemical reactions.

Recently, Professor Franklin Schultz and his co-workers at Indiana University – Purdue University at Indianapolis discovered spin-crossover coupled one-electron reduction of a number of low-spin M(III) complexes with tripodal capping ligands which are complexed to the metal through N donor atoms.[30,31] Interestingly, these redox events show unusually large enthalpy and entropy changes, as well as lowered reaction rates, that are not sufficiently explained with current physical models of redox reactions.

Our goal for the future work will be three-fold: (i) to benchmark a model chemistry by testing up to 39 functionals including LDA, GGA, meta-GGA, and hybrid functionals in combination with different choices of basis set to quantitatively reproduce their experimentally observed thermodynamics, (ii) to apply some of our understanding gleaned from this C500 project to help shed light on the physical picture which produces

these unexpected redox thermodynamics and (iii) to acquire more data to add to our knowledge of the fundamental factors that affect spin-state equilibrium including metal choice, metal oxidation state, ligand choice, ligand charge, and geometry. This joint computational and experimental endeavor will not only give me excellent experience with two very different sets of tools, but also provide us a direct feedback mechanism to test how robust the model chemistry we develop really is. Within the next year we fully expect to explore new systems computationally and hopefully drive new experimental observations through our model chemistry, and truly confirm its robustness.

V. References

(1) Gütlich, P.; Goodwin, H. A., *Top. Curr. Chem.* **2004,** *233*, 1-47.

(2) Bousseksou, A.; Molnar, G.; Matouzenko, G., *European Journal of Inorganic Chemistry* **2004**, 4353-4369.

(3) Shaik, S.; Kumar, D.; de Visser, S. P.; Altun, A.; Thiel, W., *Chem. Rev.* **2005,** *105*, 2279-2328.

(4) Nelson, K. J.; Giles, I. D.; Shum, W. W.; Arif, A. M.; Miller, J. S., *Angew. Chem. Int. Ed. Engl.* **2005,** *44*, 3129-3132.

(5) Eaton, J. P.; Nicholls, D., *Transit. Met. Chem.* **1981,** *6*, 203-206.

(6) Strassner, T.; Taige, M. A., *J. Chem. Theory Comput.* **2005,** *1*, 848-855.

(7) Jaguar 6.0, Schrödinger, Inc., Portland, Oregon, 2003.

(8) Becke, A. D., *Phys. Rev. A* **1988,** *38*, 3098-3100.

(9) Becke, A. D., *J. Chem. Phys.* **1993,** *98*, 5648-5652.

(10) Lee, C. T.; Yang, W. T.; Parr, R. G., *Phys. Rev. B* **1988,** *37*, 785-789.

(11) Vosko, S. H.; Wilk, L.; Nusair, M., *Can. J. Phys.* **1980,** *58*, 1200-1211.

(12) Hay, P. J.; Wadt, W. R., *J. Chem. Phys.* **1985,** *82*, 270-283.

(13) Wadt, W. R.; Hay, P. J., *J. Chem. Phys.* **1985,** *82*, 284-298.

(14) Hay, P. J.; Wadt, W. R., *J. Chem. Phys.* **1985,** *82*, 299-310.

(15) Baik, M.-H.; Friesner, R. A., *J. Phys. Chem. A* **2002,** *106*, 7407-7415.

(16) Dunning, T. H., Jr., *J. Chem. Phys.* **1989,** *90*, 1007-1023.

(17) Sharpe, A. G., *The chemistry of cyano complexes of the transition metals.* Academic Press: New York, 1976; p 302.

(18) Allen, F., *Acta Crystallographica Section B* **2002,** *58*, 380-388.

(19) Bruno, I. J.; Cole, J. C.; Edgington, P. R.; Kessler, M.; Macrae, C. F.; McCabe, P.; Pearson, J.; Taylor, R., *Acta Crystallographica Section B* **2002,** *58*, 389-397.

(20) Meyer, H.-J.; Pickardt, J., *Acta Crystallographica Section C* **1988,** *44*, 1715-1717.

(21) Razak, I. A.; Shanmuga Sundara Raj, S.; Fun, H.-K.; Tong, Y.-X.; Lu, Z.-L.; Kang, B.-S., *Acta Crystallographica Section C* **2000,** *56*, 291-292.

(22) Soria, D. B.; Piro, O. E.; Varetti, E. L.; Aymonino, P. J., *Journal of Chemical Crystallography* **2001,** *31*, 471-477.

(23) Antipin, M. Y.; Ilyukhin, A. B.; Kotov, V. Y., *Mendeleev Commun.* **2001**, 210-211.

(24) Antipin, M. Y.; Ilyukhin, A. B.; Kotov, V. Y.; Lokshin, B. V.; Seifer, G. B.; Chuvaev, V. F.; Yaroslavtsev, A. B., *Russian Journal of Inorganic Chemistry* **2002,** *47*, 1031-1037.

(25) Ferlay, S.; Bulach, V.; Felix, O.; Hosseini, M. W.; Planeix, J. M.; Kyritsakas, N., *Crystengcomm* **2002**, 447-453.

(26) Kotov, V. Y.; Ilyukhin, A. B., *Mendeleev Commun.* **2003**, 169-170.

(27) Malarova, M.; Kuchar, J.; Cernak, J.; Massa, W., *Acta Crystallographica Section C-Crystal Structure Communications* **2003,** *59*, M280-M282.

(28) Bie, H. Y.; Lu, J.; Yu, J. H.; Sun, Y. H.; Zhang, X.; Xu, J. Q.; Pan, L. Y.; Yang, Q. X., *J. Coord. Chem.* **2004,** *57*, 1603-1609.

(29) Hume, D. N.; Kolthoff, I. M., *J. Am. Chem. Soc.* **1943,** *65*, 1897-1901.

(30) Turner, J. W.; Schultz, F. A., *J. Phys. Chem. B* **2002,** *106*, 2009-2017.

(31) De Alwis, D. C. L.; Schultz, F. A., *Inorg. Chem.* **2003,** *42*, 3616-3622.